AIMS Energy, 11(1): 64–78.
DOI: 10.3934/energy.2023004
Received: 14 November 2022
Revised: 26 January 2023
Accepted: 31 January 2023
Published: 10 February 2023

http://www.aimspress.com/journal/energy

Research article

Preventive control method for stable operation of proton exchange membrane fuel-cell stacks

Yuto Tsuzuki[1,*], Yutaro Akimoto[2] and Keiichi Okajima[2]

[1] Graduate School of Science and Technology, University of Tsukuba, SB826,1-1-1, Tennnoudai, Tsukuba, Ibaraki,305-8573, Japan
[2] Institute of Systems and Information Engineering, University of Tsukuba, SB826,1-1-1, Tennnoudai, Tsukuba, Ibaraki, 305-8573, Japan

* **Correspondence:** Email: s2120542@s.tsukuba.ac.jp; Tel: +81-298535537.

Abstract: Flooding and dry-out are major drawback issues in proton exchange membrane fuel cells (PEMFC), which necessitate adequate prevention control techniques. In a fuel-cell stack, as flooding and dry-out occur on the inlet and outlet sides, respectively, both faults can exist simultaneously. Therefore, the timely detection of these two contradictory faults is crucial for implementing timely control measures. In this study, we propose a preventive control method that detects the fault signs early for more effective prevention. The proposed method uses a curve-fitting method, which uses overpotential as the control index. As the control index can be obtained by measuring the current, voltage, and temperature, the evaluation can be performed quickly, making it easy to implement in a PEMFC system. Under a single fault, the stack output power, hydrogen consumption, and power efficiency of the proposed preventive control method and the previous study on flooding were compared. The results showed that our preventive control method could detect flooding sooner and was superior in stack output power, hydrogen consumption, and power generation compared to the fault control method. Under conditions of mixed flooding and dry-out, both flooding and dry-out were detected using the overpotential as the control index. Thus, because the proposed method initiates control measures before the fault progresses, it is possible to ensure the continued stable operation of the fuel cells.

Keywords: PEMFC; control; flooding; dry-out; overpotential; curve fitting

1. Introduction

Proton exchange membrane fuel cells (PEMFCs) have attracted considerable interest due to their ability to exhibit high energy densities at low temperatures, compact size, high efficiency, and minimal carbon emissions. Consequently, they are used in a multitude of applications, such as fuel cell vehicles (FCVs), cogeneration systems, portable electronics, and emergency power sources [1,2]. However, the mass commercialization of PEMFCs has been hindered due to operational issues stemming from water and thermal management, such as flooding or drying out, resulting in reduced power performance and system degradation [3]. Flooding is a fault wherein the water produced during the operation of a PEMFC gets retained, thereby filling up the pores in its gas diffusion layer, which covers the reaction area of the catalyst layer and results in decreased fuel cell performance. The lower the flow rate, the greater the flooding caused by the plugging of the generated water. Correspondingly, the conductivity of the membrane is affected, and the thickness of the electrolyte changes significantly [4]. Dry-out is a fault in which the membrane dries owing to excessive operating temperatures, flow rates, and declining power. Consequently, the fuel cell membrane degrades more rapidly, causing pinholes and other defects [5].

There are several approaches to identifying the internal conditions, which include investigating the moisture state via X-ray [6], neutron tomography [7], the degree of drying of the membrane by measuring cell resistance using the current interruption method [8], and electrochemical impedance spectroscopy [9,10]. However, it is difficult to implement these methods in PEMFC systems. Fault diagnosis and control are various model-based methods [11] that delve into the reaction process of fuel cell systems and non-model-based methods by utilizing analytical models based on heuristic knowledge and signal processing techniques [12,13]. For model-based applications, Onanena et al. [14] proposed a pattern-recognition-based diagnostic approach based on electrochemical impedance spectroscopy measurements. For non-model-based approaches, Li et al. [15] used a support vector machine, and Steiner et al. [16] used neural networks to facilitate fault diagnosis. However, these methods require prior data collection, which demands time and effort to build the system.

Akimoto et al. [17] proposed a curve-fitting method that uses overpotential as a control index to diagnose and control faults. This method is easy to implement in PEMFC systems, wherein the control index can be calculated using only the initial and measured values of current, voltage, and temperature. Another advantage of this method is that it can respond to sudden faults, allowing evaluations to be performed quickly.

Despite the multiple methods proposed for implementing fault control, they are applicable only for operating conditions that cause a single fault. Each fuel cell in a stack has different internal parameters, such as gas concentration, supply pressure, and temperature. As flooding and dry-out tend to occur on the inlet and outlet side, respectively, two types of faults may coexist in a fuel-cell stack. When these happen simultaneously, purge control is used to drain water from inside the fuel cell. This quickens the drying up of the membranes in the other cells. Therefore, early detection of these two contradictory faults is necessary to control them.

In this study, we propose a preventive control method using a curve-fitting method that uses overpotential as a control index. The remainder of this paper is organized as follows. Section 2 presents the configuration of the PEMFC system used in the experiments, along with an overview of the preventive control method. Section 3 proposes a preventive control method for a single fault and compares it with a previous study. Additionally, a preventive control method was proposed for two

mixed types of flooding and dry-out faults. Finally, Section 4 summarizes the conclusions of this study.

2. Experiments and control methods

2.1. Experiments

Figure 1 shows the PEMFC and the control system. A 5-Cell PEMFC stack was used in this study. The flow channel is serpentine, and the reaction area is 37.8 cm^2. Figure 2 shows the IV curve of the PEMFC stack. In this PEMFC stack, the maximum output is 38.6 W at 15 A. For each cell voltage at 15 A, cell 1 has the higher voltage, 0.60 V and cell 4 has the lower voltage, 0.54 V. Pure hydrogen was supplied in flow mode from a cylinder, and air through a pump. A fan was installed on the stack for cooling purposes. The cell voltage, stack current, and stack temperature were converted to voltages and recorded on a personal computer (PC).

Table 1 presents the experimental conditions of this study. The faults assumed were flooding and a mixture of flooding and dry-out. Only flooding was reproduced at lower operating temperatures and flow rates. The hydrogen and air flow rates were 0.6 and 3.3 L/min, respectively. The operating temperature of the cooling fan was 45 ℃. Mixed flooding and dry-out were reproduced at higher operating temperatures and lower flow rates. The hydrogen and air flow rates were 0.4 and 1.4 L/min, respectively. These parameters for both conditions were adopted from preliminary experiments to cause the respective faults. The voltage drops due to flooding and dry-out were controlled by the flow rate and installed fan, respectively.

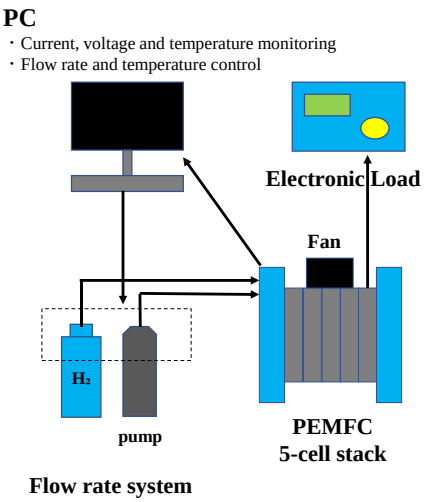

Figure 1. PEMFC and the control system.

Table 1. Experimental conditions.

Fault	Flooding	Mixed flooding and dry-out
Hydrogen [L/min]	0.6	0.4
Air [L/min]	3.3	1.4
Operating temperature [℃]	45	55–75

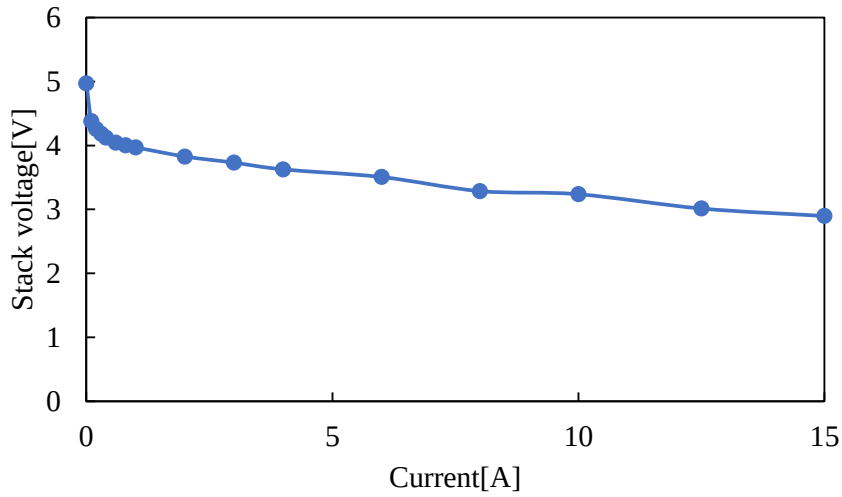

(a) Stack

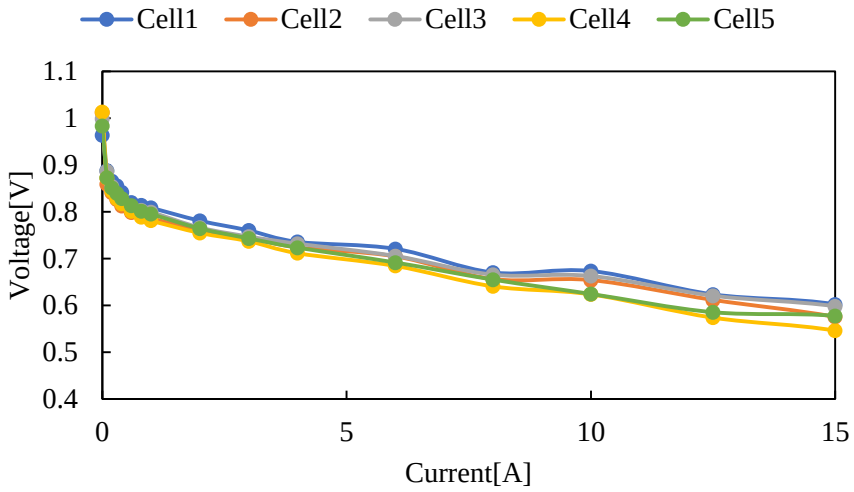

(b) Cells

Figure 2. IV curves of PEMFC stack and cells.

2.2. Control methods

2.2.1. Preventive control

Preventive control is a method to maintain power by detecting signs of faults, such as flooding and dry-out, and controlling them in advance. In this study, we propose a preventive control method that uses overpotential as a control index. Overpotential is the voltage drop associated with an increase in current density. It is classified into three types based on the factors that cause the power to drop: activation, ohmic, and concentration. The voltage drop factor can be evaluated by separating each overpotential type. The activation overpotential is the voltage drop due to the consumption of

activation energy and the reaction to become an ion. The ohmic overpotential is the voltage drop arising from the resistance to the transfer of electrons and ions in the electrolyte membrane, electrodes, separator, and other components of the fuel cell. The concentration overpotential is the voltage drop caused by a decrease in oxygen and hydrogen concentrations.

To evaluate the power reduction factor, the overpotential was calculated by fitting the curve model equation with the least-squares method based on the measured values of the cell voltage, stack current, and stack temperature obtained from the PEMFC. In this study, the curve-model equation [18] in Eq (1) was used to calculate the overpotential.

$$V = E_{0(T)} - \eta_{act(T)} - \eta_{ohmic(T)} - \eta_{con(T)} \quad (1)$$

V [V] is the cell voltage, $E_{0(T)}$ [V] is the theoretical voltage, $\eta_{act(T)}$ [V] is the activation overpotential, $\eta_{ohmic(T)}$ [V] is the ohmic overpotential, and $\eta_{con(T)}$ [V] is the concentration overpotential.

The method for calculating overpotential is described below. First, the load is gradually increased to the constant current to be used in the experiment. At that time, the values of cell voltage and stack temperature corresponding to the preset current are recorded. In addition, the cell voltage and stack temperature during constant current operation, which are updated every second, are used for fitting and IV curves are predicted to calculate each overpotential. These overpotentials were calculated by PC in Figure 1 using measuring value of PEMFC stack at every second.

Several equations have been proposed in previous studies on curve models, with the simplest by Kim et al. [19]. Squadrito et al. [20] proposed an equation that used the power of the current density as a factor in the concentration overpotential term to accommodate the steep voltage. However, these assume constant temperature and humidity, while the curve model equation employed herein uses temperature as a variable for all overpotential terms. Thus, it can be considered appropriate for actual system implementation because the temperature of the fuel cells changes during the operation phase.

2.2.2. Control strategy

In Section 3, the method proposed herein is compared with that in a previous study [17] for a single fault. Subsequently, the proposed control method under mixed flooding and dry-out conditions was adopted.

Figure 3 shows the control flow in the preventive and fault-control strategies employed against flooding. After starting the constant-current operation, the overpotential was calculated every second. The concentration overpotential was used as a control index since flooding is caused by it. Control was exercised when the concentration overpotential exceeded the control threshold. In this experiment, the control threshold was set to 15% of the theoretical voltage $E_{0(T)}$. The control method is not a purge as in fault control, but rather the flow rate of hydrogen and air is increased every 2 seconds by 0.2 and 0.6 L/min, respectively, and when concentration overpotential is no longer calculated (0.001 V), the control is finished and the flow rate returns to the initial flow conditions.

The fault control method used for comparison was adopted from a previous study [17]. The control method involved a second hydrogen and air purge (20 L/min) when the threshold value was lowered. The experiment was conducted at a constant-current operation for 30 min, and four parameters were compared: the control frequency, stack output, hydrogen consumption, and power efficiency. The calculation of efficiency is described in Eq (2).

$$\eta_{LHV} = \frac{W}{C \times \Delta H^0} \times 100 \quad (2)$$

where η_{LHV} [%] represents the power efficiency (Lower Heating Value), W [W] is the stack power, C [mol/s] represents the fuel consumption, and ΔH^0 [kJ/mol] represents the standard enthalpy of the reaction.

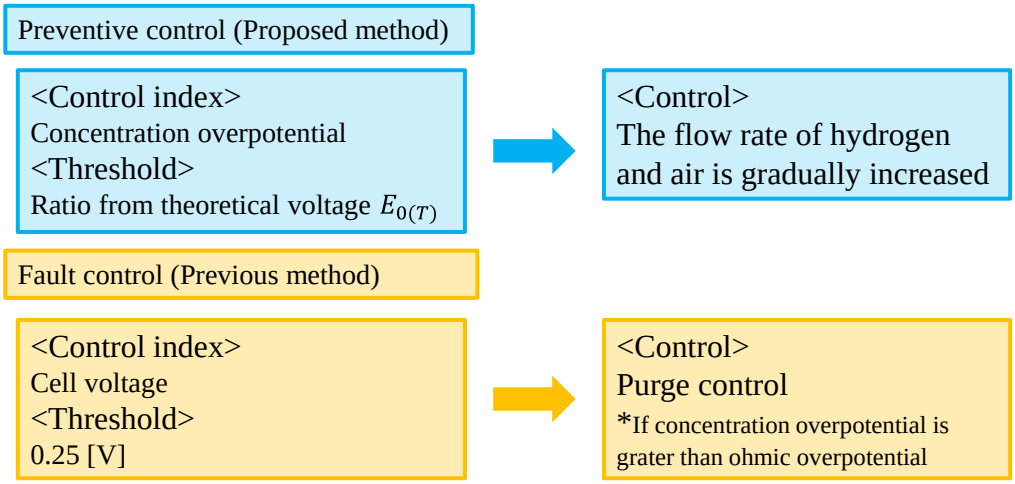

Figure 3. Outline of the proposed and previous method of flooding.

Figure 4 shows the control flow of the preventive control strategy for a mixture of flooding and dry-out. Concentration overpotential was used as the control index to control the flooding. The control threshold 1 in Figure 3 was set at 10% of the theoretical voltage $E_{0(T)}$ to detect dry-out more quickly. The control method would increase the hydrogen and air flow rates by 0.2 and 0.6 L/min, respectively, every 5 seconds until the concentration overpotential fell below the control threshold.

Dry-out is caused by the ohmic overpotential, which is used as the control index. The evaluation method records the initial ohmic overpotential after starting a constant-current operation and calculates the difference from the ohmic overpotential during operation. This difference is used as the control threshold 2 in Figure 3. This is because the ohmic overpotential is proportional to the current value; therefore, its value changes depending on the current during the operational phase. The control threshold of ohmic overpotential in this experiment was set to 0.075 V. When the value exceeded the control threshold, the fan cooled the temperature down to 60 °C, and when it fell below the control threshold, preventive control was suspended.

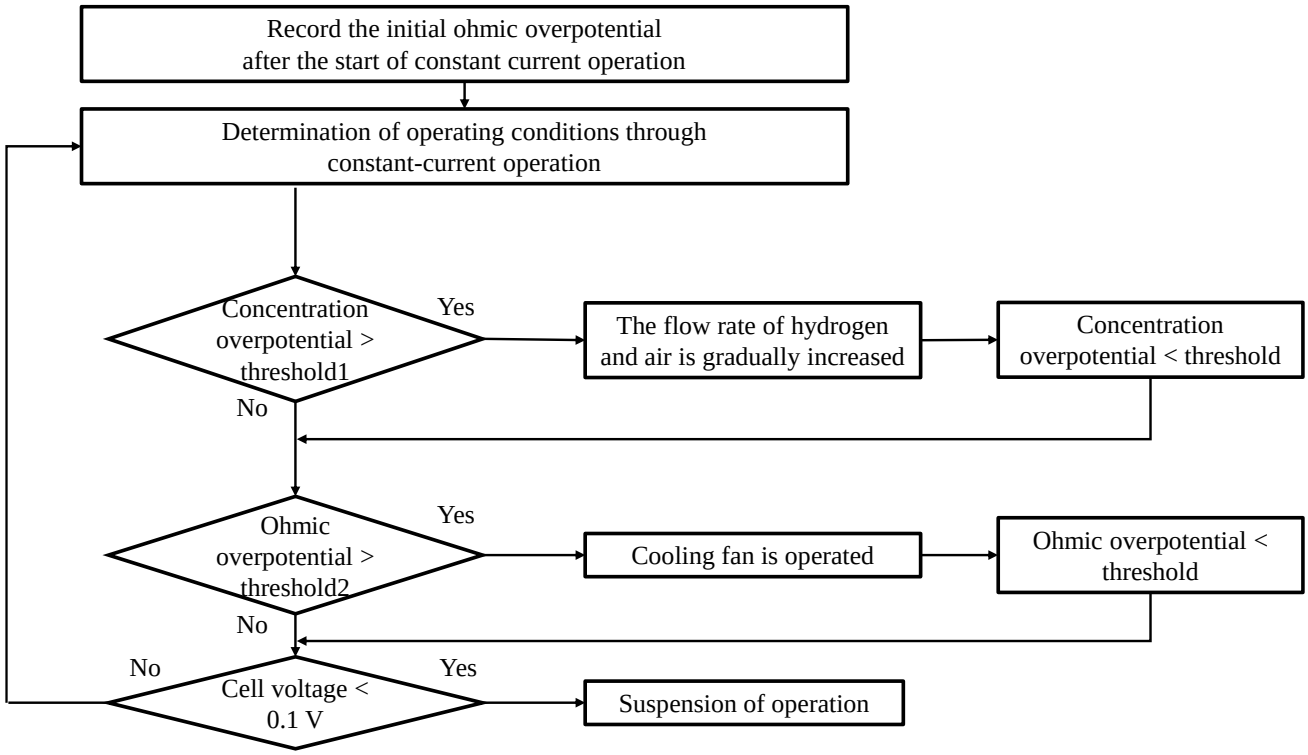

Figure 4. Control flowchart to prevent mixed flooding and dry-out.

3. Results and discussion

3.1. Comparison between the proposed method and previous study for single fault

Figure 5 shows the transition of Cell 4 voltage in preventive and fault control methods. In this stack, flooding was often detected in Cell 4. Flooding is detected at cell voltages around 0.25 V in fault control method, whereas in the preventive control method, it is detected at cell voltages around 0.45 V, which restrain the cell voltage drop.

Figure 6 compares the hydrogen and air flow rates, Cell 4 voltage and concentration overpotential, in the preventive control method from 1400 to 1500 s. From 1400 s, the concentration overpotential increased as the cell voltage decreased and reached the control threshold at 1448 s. At 1400 s, the cell voltage and concentration overpotential were 0.556 and 0.029 V, respectively. The control measures were implemented at 1449 and 1457 s. When the cell voltage increased (0.602 V) and the concentration overpotential decreased (5.65×10^{-5} V), the control measures were suspended.

Table 2 shows the efficiency and parameters of each control method during the constant-current operation. The control frequency is higher for the preventive control method at 54 times and the fault control method at 6 times, but the stack output power is higher and the hydrogen consumption is lower than that of the fault control method. The efficiency of the preventive control method was 1.4% higher than that of the fault control method at 26.5%, compared to 25.1% for the fault control method.

Based on these results, the proposed method detects flooding earlier than the fault control method using the concentration overpotential as a control index. Therefore, it has the advantage of average output power. Additionally, the operation could be performed while increasing the power efficiency as hydrogen consumption was suppressed by gradually increasing the flow rate unlike the purge control

method used in the previous study.

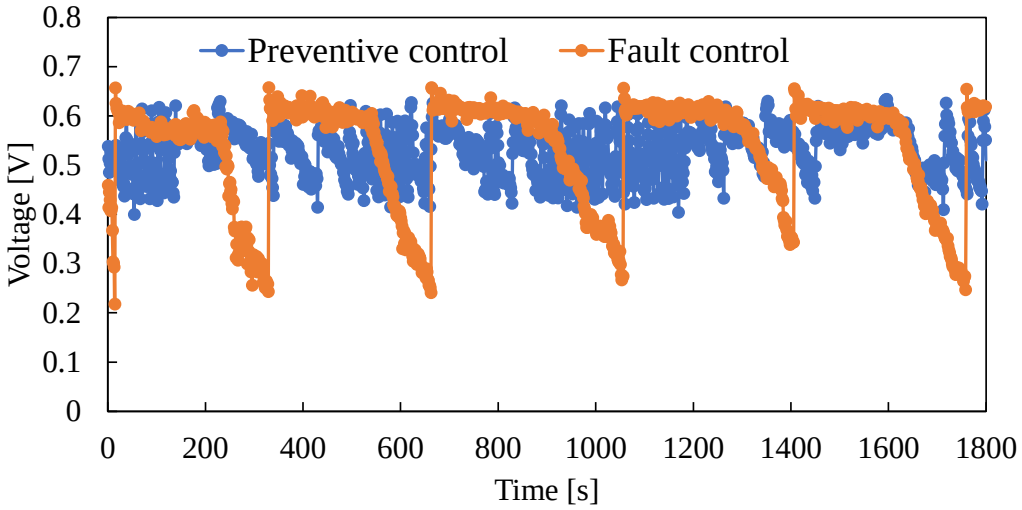

Figure 5. Comparison of Cell 4 voltage in preventive and fault control.

Table 2. Comparison of proposed and previous study method.

Method	Preventive control	Fault control
Control frequency [Times]	54	6
Average power output [W]	30.7	30.1
Hydrogen consumption [L]	19.4	19.9
Efficiency [%]	26.5	25.1

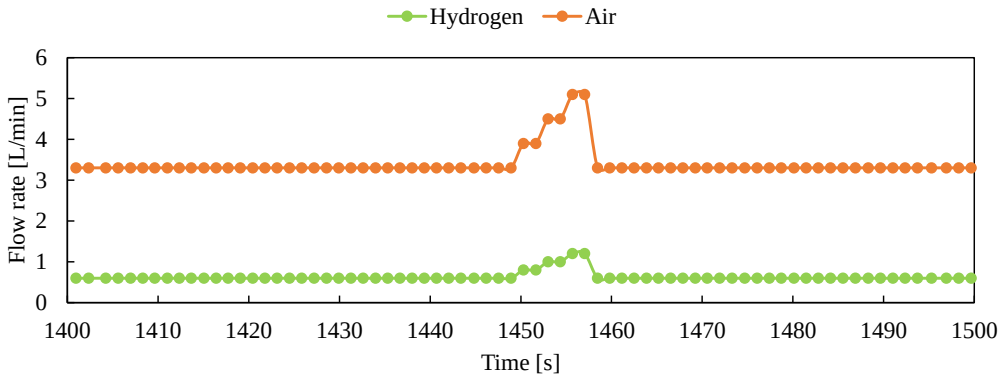

(a) Hydrogen and air flow rates.

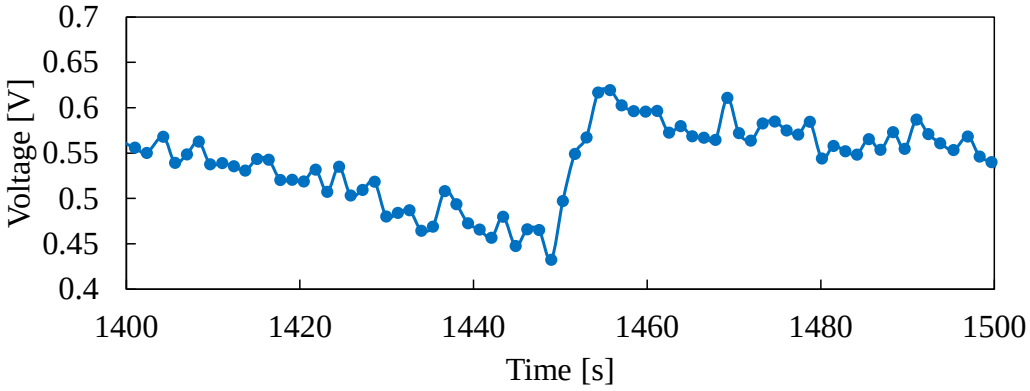

(b) Cell voltage.

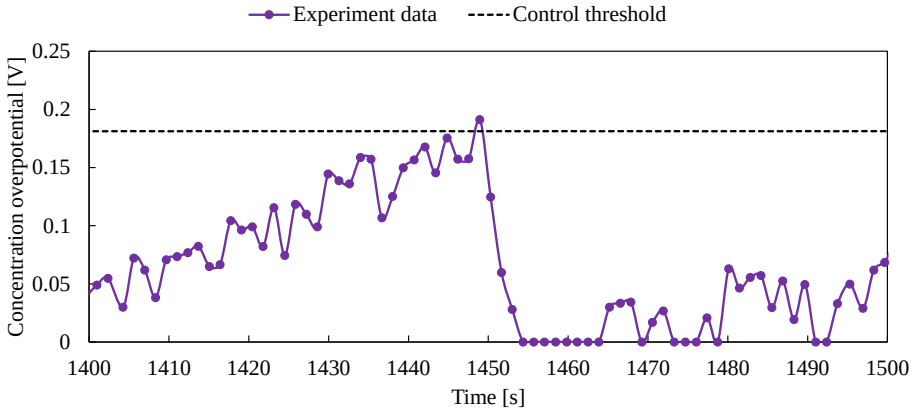

(c) Concentration overpotential.

Figure 6. Hydrogen, air flow rate, Cell 4 voltage, and concentration overpotential in the preventive control method from 1400 to 1500 seconds.

3.2. Preventive control of mixed faults in the proposed method

Figure 7 shows the voltage and temperature transitions for all the cells under the preventive control method. All cells were maintained at the voltage of 0.35 V until 1100 seconds. Table 3 shows number of control frequency for the proposed method. In this experiment, dry-out was detected 7 times and flooding was detected 3 times. Figure 8 shows the voltage and ohmic overpotential of Cell 2 with temperature and dry-out control from 400 to 1000 s. The dry-out was detected three times: from 539 to 650 s, from 758 to 816 s, and from 860 to 927 s. The initial ohmic overpotential of Cell 2 in this experiment was 0.137 V. As the temperature increased from 400 to 539 s, the cell voltage decreased from 0.438 to 0.372 V, and the ohmic overpotential increased from 0.164 to 0.220 V. From 539 to 650 s, the fan was controlled to suppress the decrease in cell voltage. This behavior is evident from 813 to 927 s: from 813 to 860 s, the temperature increases from 62.2 ℃ to 67.7 ℃, the Cell voltage decreases from 0.425 to 0.392 V, and the ohmic overpotential increases from 0.194 to 0.210 V. From 860 to 927 s,

fan control increased the cell voltage to 0.440 V and decreased the ohmic overpotential to 0.183 V.

Because stable operation was possible with the cooling fan during all periods, it is considered that the membrane got dried when operating at a high temperature. The difference in the internal condition of the stack before control was considered to be the cause of the output increase due to the cooling fan during the third control at 860–927 s. In this experiment, dry-out was detected for the first time at 539–650 s. Moreover, the fan control involves temporary cooling. Therefore, from the second detection onwards, residual heat remained in the stack compared to the first control at 539–650 s, so the membrane was more likely to dry. Furthermore, the fact that the stack temperature rises earlier after the second control at 758–816 s also indicates that the latter is drying the membrane. Consequently, the control frequency of the cooling fan also increased, prompting an increase in the cell voltage during the third control at 860–927 s. Furthermore, the voltage of Cell 5 was 0.477 V at 758 s, but increased to 0.512 V at 927 s due to the cooling fan control.

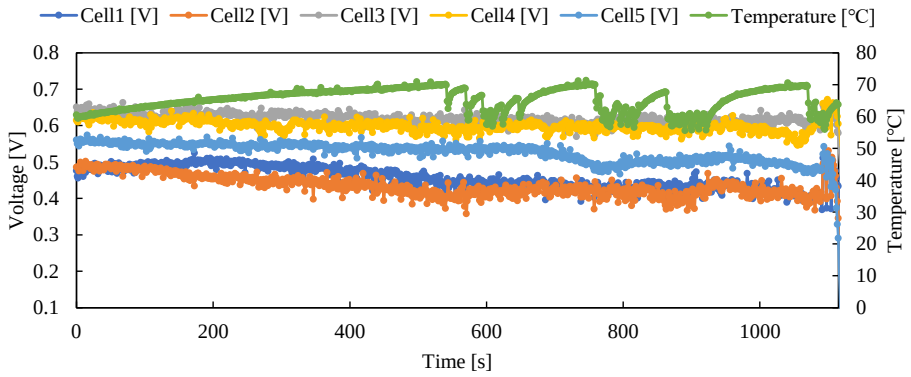

Figure 7. Comparison of each cell voltage and stack temperature.

Table 3. Comparison of each failure control frequency in proposed method.

Method	Preventive control
Control frequency of dry-out [Times]	7
Control frequency of flooding [Times]	3

Figure 9 shows the voltage and concentration overpotential of Cell 1 with hydrogen, airflow, and flooding control from 950 to 1115 s. At 1091 s, the concentration overpotential exceeds the control threshold for the first time. The cell voltage and concentration overpotential in Cell 1 were 0.369 and 0.152 V, respectively. The cell voltage increased at 0.511 V, and the concentration overpotential at 3.68×10^{-5} V decreased via flow rate control. The cell voltage is increased by controlling the flow rate. However, at the third control time, despite the increase in cell voltage, the flow control continued, and the voltage dropped. This was because flooding was detected in other cells. Figure 10 shows the voltage and concentration overpotentials of cell 5 from 1090 to 1115 s. The concentration overpotential exceeded the control threshold of 1104 second. Control was initiated, and the cell voltage increased at 1105 s, but then gradually decreased. It is thought that the cell membrane accelerated drying via the continued flow rate control.

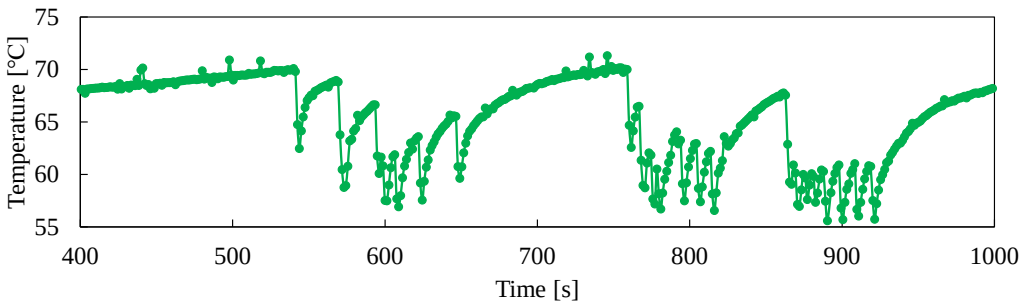

(a) Temperature.

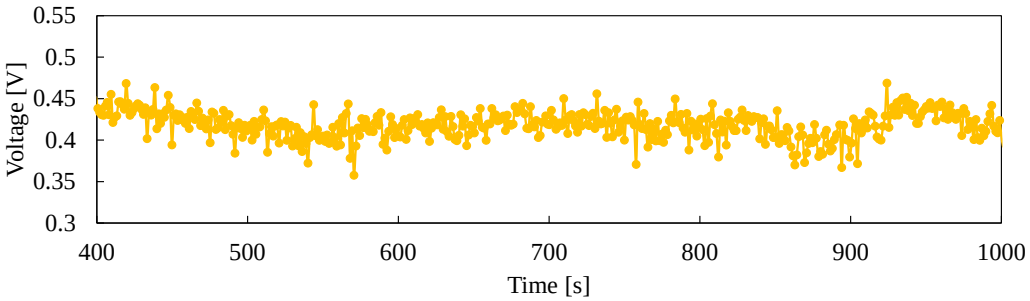

(b) Cell voltage.

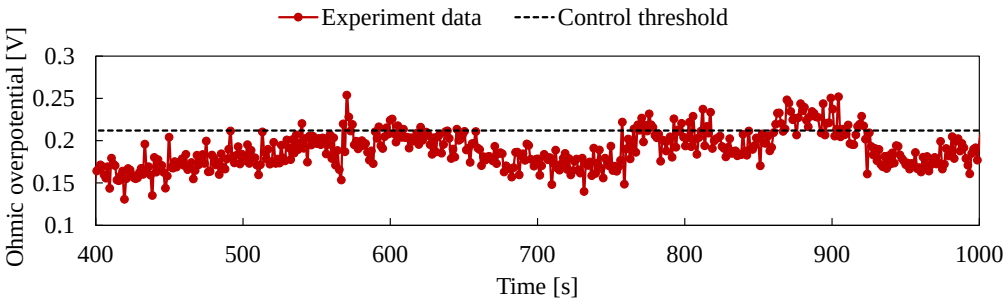

(c) Ohmic overpotential.

Figure 8. Stack temperature, Cell 2 voltage, ohmic overpotential from 400 to 1000 s.

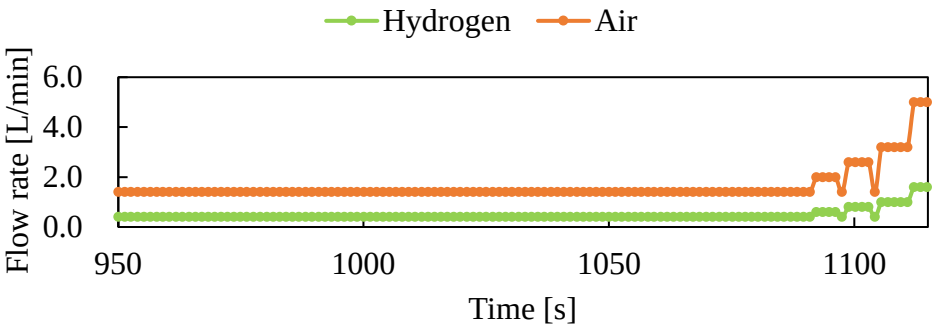

(a) Hydrogen and air flow rates.

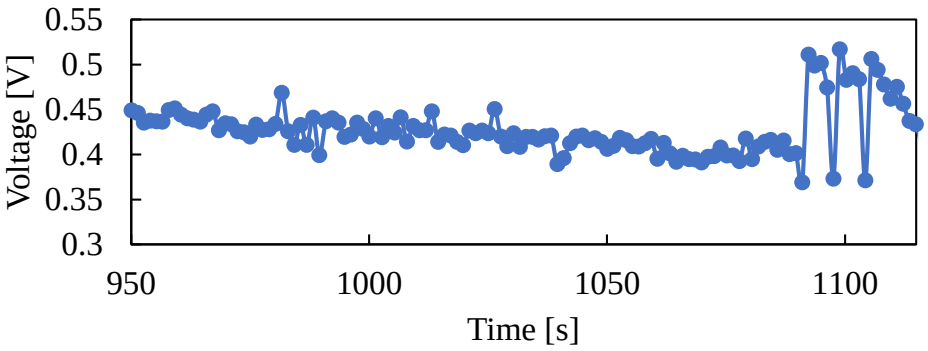

(b) Cell voltage.

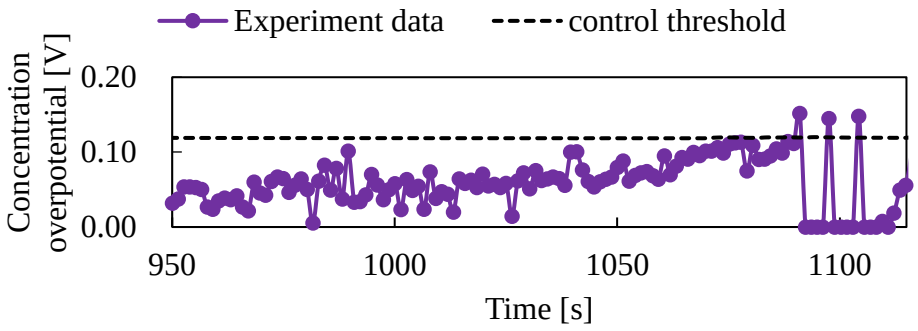

(c) Concentration overpotential.

Figure 9. Hydrogen, air flow rate, Cell 1 voltage, and concentration overpotential from 950 to 1115 s.

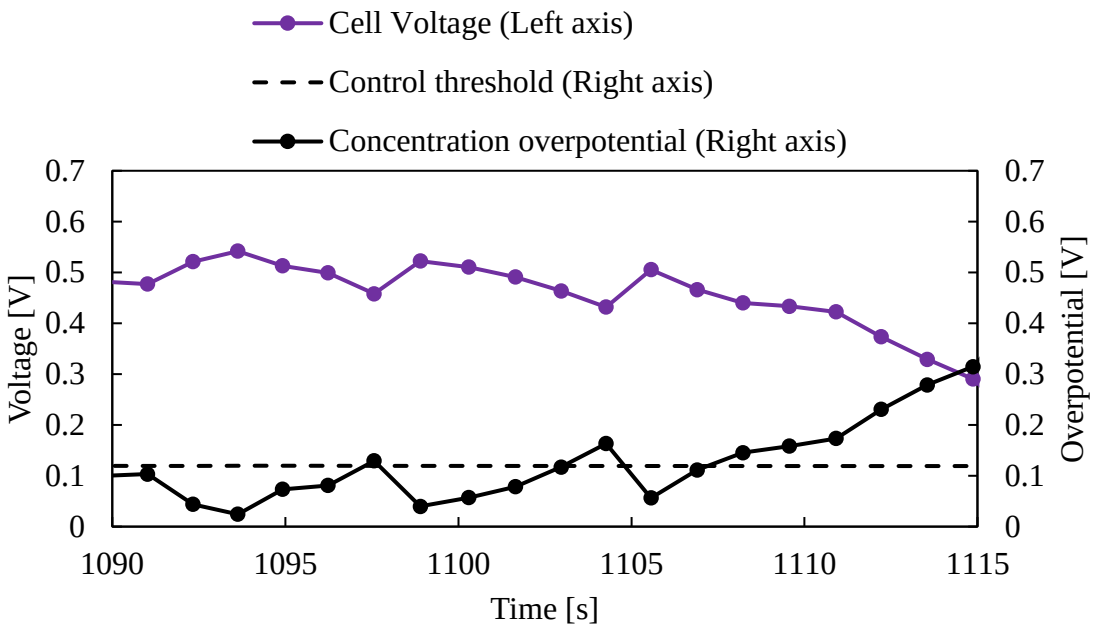

Figure 10. Cell 5 voltage and concentration overpotential from 1090 to 1115 s.

4. Conclusions

In this study, a preventive control method using overpotential as a control index was proposed that can diagnose and avoid contradictory faults in the stack to ensure stable operation of the fuel cell systems. The proposed method is easy to implement in a PEMFC system because the control index can be calculated by measuring the current, voltage, and temperature and can be evaluated quickly.

For a single fault, we compared the method proposed in this study with a previous study on flooding. The preventive control method detected flooding earlier than the fault control method by using the concentration overpotential as the control index and improved the voltage of Cell 4. Additionally, although the control frequency increased, hydrogen consumption was suppressed by gradually increasing the flow rate unlike the purging control method. Furthermore, the system was superior in terms of the stack power output and power efficiency. This showed that not only could faults be avoided in advance, but the system could also be operated while improving the power efficiency.

Under conditions of mixed flooding and dry-out, both flooding and dry-out were detected using the concentration overpotential for flooding and the difference between the ohmic overpotential after the start and during operation, as the control index for dry-out. The voltage of Cell 1 was improved for flooding, and that of Cell 2 was improved for dry-out. As a result, we were able to maintain more than 0.35 V in all cells until 1100 seconds.

From these results, because the proposed method initiates control measures before the fault progresses, stable operation is possible. Furthermore, it can be integrated with other control systems, increasing the reliability of the fuel cell system.

Acknowledgments

This research was supported by the Iwatani Naoji Foundation, TEPCO Memorial Foundation research grant and the Mazda Foundation research grant.

Conflict of interest

The authors declare no conflict of interest.

References

1. Ritzberger D, Hametner C, Jakubek S (2020) A real-time dynamic fuel cell system simulation for model-based diagnostics and control: Validation on real driving data. *Energies* 13: 3148. https://doi.org/10.3390/en13123148
2. Bizon N, Mazare G, Ionescu M, et al. (2018) Optimization of the proton exchange membrane fuel cell hybrid power system for residential buildings. *Energy Convers Manage* 163: 22–37. https://doi.org/10.1016/j.enconman.2018.02.025
3. Yang B, Wang J, Yu L, et al. (2020) A critical survey on proton exchange membrane fuel cell parameter estimation using meta-heuristic algorithms. *J Cleaner Prod* 265: 121660. https://doi.org/10.1016/j.jclepro.2020.121660
4. Mason T, Millichamp J, Neville T, et al. (2013) A study of the effect of water management and electrode flooding on the dimensional change of polymer electrolyte fuel cells. *J Power Sour* 242: 70–77. https://doi.org/10.1016/j.jpowsour.2013.05.045
5. Barbir F, Gorgun H, Wang X (2005) Relationship between pressure drop and cell resistance as a diagnostic tool for PEM fuel cells. *J Power Sour* 141: 96–101. https://doi.org/10.1016/j.jpowsour.2004.08.055
6. Chevalier S, Ge N, George M, et al. (2017) Synchrotron X-ray radiography as a highly precise and accurate method for measuring the spatial distribution of liquid water in operating polymer electrolyte membrane fuel cells. *J Electrochem Soc* 164: F107–F114. Available from: https://iopscience.iop.org/article/10.1149/2.0041702jes.
7. Alrwashdeh S, Alsaraireh F, Saraireh M, et al. (2018) In-situ investigation of water distribution in polymer electrolyte membrane fuel cells using high-resolution neutron tomography with 6.5 μm pixel size. *AIMS Energy* 6: 607-614. https://doi.org/10.3934/energy.2018.4.607
8. Rubio M, Urquia A, Dormido S (2007) Diagnosis of PEM fuel cells through current interruption. *J Power Sour* 171:670–677. https://doi.org/10.1016/j.jpowsour.2007.06.072
9. Jullian G, Cadet C, Rosini S, et al. (2020) Fault detection and isolation for proton exchange membrane fuel cell using impedance measurements and Multiphysics modeling. *Fuel Cells* 20: 558–569. https://doi.org/10.1002/fuce.202000022
10. Canut J, Abouatallah R, Harrington D. (2006) Detection of membrane drying, fuel cell flooding, and anode catalyst poisoning on PEMFC stacks by electrochemical impedance spectroscopy. *J Electrochem Soc*153: A857–A864. Available from: https://iopscience.iop.org/article/10.1149/1.2179200.

11. Saygili Y, Eroglu I, Kincal S (2015) Model based temperature controller development for water cooled PEM fuel cell systems. *Int J Hydrogen Energy* 40: 615–622. https://doi.org/10.1016/j.ijhydene.2014.10.047
12. Cadet C, Jemeï S, Druart F, et al. (2014) Diagnostic tools for PEMFCs: From conception to implementation. *Int J Hydrogen Energy* 39: 10613–10626. https://doi.org/10.1016/j.ijhydene.2014.04.163
13. Wang J, Yang B, Zeng C, et al. (2021) Recent advances and summarization of fault diagnosis techniques for proton exchange membrane fuel cell systems: A critical overview. *J Power Sour* 500: 229932. https://doi.org/10.1016/j.jpowsour.2021.229932
14. Onanena R, Oukhellou L, Côme E, et al. (2012) Fault-diagnosis of PEM fuel cells using electrochemical spectroscopy impedance. *IFAC Proc* 45: 651–656. Available from: https://hal.archives-ouvertes.fr/hal-03223601.
15. Li Z, Outbib R, Giurgea S, et al. (2019) Fault diagnosis for fuel cell systems: A data-driven approach using high-precise voltage sensors. *Renewable Energy* 135: 1435–1444. https://doi.org/10.1016/j.renene.2018.09.077
16. Steiner Y, Hissel D, Moçotéguy P (2011) Diagnosis of polymer electrolyte fuel cells failure modes (flooding & drying out) by neural networks modeling. *Int J Hydrogen Energy* 36: 3067–3075. https://doi.org/10.1016/j.ijhydene.2010.10.077
17. Akimoto Y, Okajima K (2021) Simple on-board fault-detection method for proton exchange membrane fuel cell stacks using by semi-empirical curve fitting. *Appl Energy* 303: 17654. https://doi.org/10.1016/j.apenergy.2021.117654
18. Akimoto Y, Okajima K (2014) Semi-empirical equation of PEMFC considering operation temperature. *Energy Technol Policy* 1: 91–96. https://doi.org/10.1080/23317000.2014.972480
19. Kim J, Lee M, Srinivasan S, et al. (1995) Modeling of proton exchange membrane fuel cell performance with an empirical equation. *J Electrochem Soc* 142: 2670–2674. https://doi.org/10.1149/1.2050072
20. Squadrito G, Maggio G, Passalacqua E, et al. (1999) An empirical equation for polymer electrolyte fuel cell (PEFC) behaviour. *J Appl Electrochem* 29: 1449–1455. Available from: https://link.springer.com/article/10.1023/A:1003890219394.